



Thermodynamic interpretation of secondary ion and photon emission during sputtering of silicon
by Ronald Albert Burghard

A thesis submitted in partial fulfillment of the requirements for the degree of DOCTOR OF
PHILOSOPHY in Physics
Montana State University
© Copyright by Ronald Albert Burghard (1977)

Abstract:

Secondary ion mass spectrometry (SIMS) and sputter-induced photon emission (SIPE) data have been analyzed using local thermodynamic equilibrium (LTE) models.

The secondary ion model used was that proposed by Andersen and Hinthorne, which uses the Saha-Eggert equation. The photon emission data were analyzed using LTE plasma equations for photon emission. The data were obtained from silicon samples doped with boron, phosphorus, and arsenic, using argon, nitrogen, and oxygen beams.

The existence of LTE at the surface of solids during sputtering can be checked by comparing the temperatures obtained from the secondary ions with those obtained from the photons emitted. The temperatures obtained from the secondary ion data were 8400°K for N_2^+ bombardment and 11,000°K for O_2^+ bombardment. The temperatures obtained from the photon emission data were 4240°K, 4860°K, and 4450°K for argon, nitrogen, and oxygen bombardment, respectively. Thus, LTE does not appear to exist at the surface of solids during sputtering.

© 1978

RONALD ALBERT BURGHARD

ALL RIGHTS RESERVED

THERMODYNAMIC INTERPRETATION OF SECONDARY ION
AND PHOTON EMISSION DURING SPUTTERING
OF SILICON

by

RONALD ALBERT BURGHARD

A thesis submitted in partial fulfillment
of the requirements for the degree

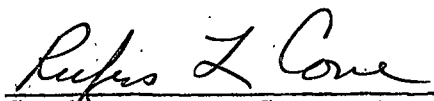
of

DOCTOR OF PHILOSOPHY

in

Physics

Approved:


Chairperson, Graduate Committee


Head, Major Department


Graduate Dean

MONTANA STATE UNIVERSITY
Bozeman, Montana

December, 1977

ACKNOWLEDGMENTS

The author is very grateful for the support of the National Science Foundation through an energy traineeship.

A special thanks is extended to the many people who made this study possible. Jim Guthrie, Garth Fahrback, and Jim Foesch at Sandia Labs were very involved and helpful in obtaining the IMMA data. Special thanks go to Bill Spencer and Bob Gregory of Sandia Labs, who through their generosity with the equipment, were very instrumental in initiating this study.

The assistance and encouragement of Wendland Beezhold, Bob Swenson, Gerald Lapeyre, John Hanton, Ed Kelley, and Mark Baldwin are gratefully acknowledged. A very special thanks is extended to Rufus Cone, who as my thesis advisor had the difficult task of helping me complete this program.

The support and encouragement of my parents, Al and Gladys Burghard, and my wife's parents, John and Lillian Laws, is acknowledged with a great deal of thanks. My thanks to Sharon for her support throughout the program and help in editing and typing the manuscript cannot be overstated.

TABLE OF CONTENTS

	Page
VITA	iii
ACKNOWLEDGMENT	iv
LIST OF TABLES	vii
LIST OF FIGURES	viii
ABSTRACT	xi
I. INTRODUCTION	1
II. BACKGROUND	6
A. Sputtering	6
B. Ion Emission During Ion Bombardment	9
1. Experimental Data	9
2. Quantum Mechanical Surface Models	11
3. Thermodynamic Models	12
4. Summary of Ion Emission Theories	19
C. Photon Emission During Ion Bombardment	20
1. Experimental Data	20
2. Present Theories on Photon Emission	24
III. EXPERIMENTAL EQUIPMENT AND PROCEDURES	27
A. Secondary Ion Emission	27
B. Sputter-Induced Photon Emission System	30
IV. EXPERIMENTAL RESULTS AND DISCUSSION	36
A. Secondary Ion Emission	36
1. Experimental results	36
2. Data Analysis	50
B. Photon Emission	69
1. Experimental Results	69
2. Data Analysis	82
C. Discussion	97

	Page
V. SUMMARY	102
APPENDICES	106
REFERENCES	135

LIST OF TABLES

Table	Page
I. Count rate data and atomic concentrations	51
II. CARISMA using N_2^+ data with B and P.	59
III. CARISMA using N_2^+ data with B and P (x3)	60
IV. CARISMA using O_2^+ data with B and P	62
V. CARISMA using O_2^+ data with B and P (x3)	66
VI. Detector currents of Si I lines.	83
VII. Transition probability data.	86
VIII. CARISMA using N_2^+ data	114
IX. CARISMA using N_2^+ data (P^+x3).	115
X. CARISMA using O_2^+ data	116
XI. CARISMA using O_2^+ data (P^+x3).	117
XII. CARISMA using O_2^+ data (SiO^+).	118
XIII. CARISMA using O_2^+ data (SiO^+, P^+x3)	119

LIST OF FIGURES

Figure	Page
1. Relative secondary ion currents	10
2. Surface electron transition models.	13
3. Thermionic emission process	18
4. Line width of Si I 2882 Å line.	22
5. Emission intensity of Si I 2882 Å line.	23
6. Schematic of IMMA system.	28
7. Photon emission equipment	31
8. Mass scan of silicon bombarded with N_2^+	37
9. Mass scan of silicon bombarded with O_2^+	40
10. Arsenic profile in silicon.	41
11. Boron profile in silicon using N_2^+ beam	44
12. Boron profile in silicon using O_2^+ beam	46
13. Phosphorus profile in silicon using N_2^+ beam	48
14. Phosphorus profile in silicon using O_2^+ beam	49
15. Region of $\log P_e$ and T	54
16. $\log P_e$ versus T dependence.	57
17. $\ln(IQ^0/C^*Q^+)$ versus ionization energy	64
18. Ionization energy levels	67
19. Spectrum for 20 keV argon beam	71
20. Spectrum for 20 keV nitrogen beam	72

Figure	Page
21. Spectrum for 20 keV oxygen beam	73
22. Ratio of Si II and Si III lines for argon beam	75
23. Ratio of Si II and Si III lines for nitrogen beam	76
24. Ratio of Si II and Si III lines for oxygen beam	77
25. Ratio of Si I lines for argon beam.	78
26. Ratio of Si I lines for nitrogen beam	79
27. Ratio of Si I lines for oxygen beam	80
28. $\ln(I\lambda^3/gf)$ versus energy for argon beam.	87
29. $\ln(I\lambda^3/gf)$ versus energy for nitrogen beam	88
30. $\ln(I\lambda^3/gf)$ versus energy for oxygen beam	89
31. $\ln(I\lambda^3/gf)$ versus energy	91
32. Energy levels for Si I lines	93
33. Partition function ratios	122
34. α -values for boron	123
35. α -values for nitrogen	124
36. α -values for oxygen	125
37. α -values for silicon	126
38. α -values for phosphorus	127
39. α -values for arsenic	128

Figure		Page
40.	β -values for boron	129
41.	β -values for nitrogen	130
42.	β -values for oxygen	131
43.	β -values for silicon	132
44.	β -values for phosphorus	133
45.	β -values for arsenic	134

ABSTRACT

Secondary ion mass spectrometry (SIMS) and sputter-induced photon emission (SIPE) data have been analyzed using local thermodynamic equilibrium (LTE) models. The secondary ion model used was that proposed by Andersen and Hinthorne, which uses the Saha-Eggert equation. The photon emission data were analyzed using LTE plasma equations for photon emission. The data were obtained from silicon samples doped with boron, phosphorus, and arsenic, using argon, nitrogen, and oxygen beams.

The existence of LTE at the surface of solids during sputtering can be checked by comparing the temperatures obtained from the secondary ions with those obtained from the photons emitted. The temperatures obtained from the secondary ion data were 8400°K for N₂⁺ bombardment and 11,000°K for O₂⁺ bombardment. The temperatures obtained from the photon emission data were 4240°K, 4860°K, and 4450°K for argon, nitrogen, and oxygen bombardment, respectively. Thus, LTE does not appear to exist at the surface of solids during sputtering.

I. INTRODUCTION

Surface chemical analysis techniques have been developed recently using the particles emitted during low energy (<30 keV) ion bombardment of solids. Erosion of the solid surface occurs¹⁻³ during such bombardment and is usually referred to as sputtering. The particles emitted from the surface of the solid during sputtering include backscattered primary beam ions, secondary atoms, ions, and molecules from the solid, electrons, and photons. This study will explore quantitative aspects of the secondary ion emission and photon emission techniques.

The use of secondary ion mass spectroscopy (SIMS) in chemical analysis of solids has developed rapidly since the introduction of the ion microscope by Castaing and Slodzian,⁴ and many different SIMS systems have been developed. These include the ion microprobe,⁵ the ion microprobe mass analyzer,⁶ and the static SIMS.⁷ A comprehensive review of these up to 1974 is given by Liebl.^{8,9} These SIMS systems typically consist of an ion source to create the ions which bombard the solid,

a secondary ion energy filter, and a mass spectrometer with detector. The energy filter is necessary if one is to obtain high mass resolution, since the energy of the secondary ions can vary from a few eV to hundreds of eV. Quadrupole mass spectrometers have been widely adopted for the mass spectrometer component.

A second related techniques referred to as sputter-induced photon emission (SIPE) has been promoted as a chemical analysis technique by White, Tolk and Simms,^{10,11} and Tsong.^{12,13} The systems typically include an ion source, monochromator, and photomultiplier detector. The light emitted during low energy ion bombardment of solids includes infra-red, visible, ultraviolet, and vacuum ultraviolet light. Most of this light appears to originate from the excited states of sputtered atoms, ions, and molecules which decay via photon emission after leaving the solid. Other light, such as background radiation^{14,15} and light from atoms excited under channeling conditions,¹⁶ also appears to originate from molecules and atoms which have left the surface. Zivitz and Thomas,¹⁷ however, explain the background radiation using a model for

surface decay.

Both SIMS and SIPE techniques have been found to be valuable in determining the chemical composition of solids.^{13,18-20} Using SIMS, one is able to detect almost any elements in a solid. The detection limit can be as low as parts per billion for some elements, while depth resolution can be as good as 10-50 Å, and the surface areas analyzed can be as small as 2 μm in diameter. With SIPE, one can obtain similar depth resolution, but SIPE cannot typically detect as low a concentration as the SIMS techniques.

Although the two techniques offer much chemical information on solids, their usefulness in analyzing unknown materials has suffered greatly from the lack of an acceptable method for relating experimental observations to surface concentrations of the atoms.^{13,21-26} In order for the techniques to reveal quantitative chemical information, a much better understanding of the processes involved in creating the ions and excited atoms must be obtained.

One presently available model, which was developed by Andersen and Hinthorne,²⁷ assumes that the sputtered

particles are emitted from a region of high temperature that is in local thermodynamic equilibrium (LTE). Plasma equations developed for LTE are then applied to predict the concentrations of elements in the original solid from sputtered ion data. The model has been used extensively by Andersen and Hinthorne on a wide assortment of materials, and the predictions match the known concentrations of many elements reasonably well.²⁸

Although their model is more capable of quantitative predictions than any other present model, an adequate understanding of why the model should explain sputtered ion yields does not presently exist. The intent of this study is to compare the temperatures obtained from secondary ion emission with those obtained from sputter-induced photon emission. If LTE exists on the surface, photons emitted from excited sputtered atoms should also be governed by the plasma equations under LTE. The experiments reported here allow a critical test of the hypothesis that LTE exists for silicon samples bombarded with argon, nitrogen and oxygen beams.

Temperatures were predicted from both secondary

ion emission data and photon emission data. The temperatures from the secondary ion emission data were obtained using the known concentrations of impurities in the silicon samples. The calculations were performed by the computer program CARISMA, which was written by Andersen and Hinthorne. The temperatures from photon emission data were obtained by comparing the relative intensities of the Si I lines. The temperatures obtained from ion emission and from photon emission differed by a factor of approximately two.

In order to put the present work in perspective, a review of sputtering models, secondary ion emission, and photon emission is given in Chap. II. The equipment used during this study is discussed in Chap. III. The experimental results and discussion are contained in Chap. IV, while Chap. V summarizes the results and conclusions of this study. Additional secondary ion emission models are summarized in Appendix A, while the calculations using the computer program CARISMA are discussed in Appendix B.

II. BACKGROUND

The development of models to predict the sputtering ratios (number of target atoms emitted/incident ion) has progressed rapidly in the past twenty years. These models have become well accepted, and the predictions using these models are fairly accurate. The models used to predict secondary ions and photons during ion bombardment are, however, much less accurate, less accepted, and much less understood.

This chapter includes a discussion of sputtering, secondary ion emission, and photon emission during ion bombardment of solids. The sputtering ratio models relevant to the ion beam conditions of this study are discussed in Section A. The secondary ion models considered during this study are discussed in Section B, while other secondary ion models are summarized in Appendix A. The chapter is completed with a discussion of photon emission in Section C.

A. Sputtering

A unified theory of sputtering which describes experimental data for all energies of the incident ion

beam has yet to be developed. Rather, the analysis of sputtering has developed through models which tend to fit a specific region of incident energy.^{1,2} The region of interest for this study is from 5 keV to 20 keV incident energies, using O_2^+ , N_2^+ and Ar^+ ion beams. Two sputtering models which have been used extensively in this region of energy were developed by Rol et al.²⁹ and Sigmund.³⁰ Additional information of interest has been given by other investigators.³¹⁻³⁵

The model proposed by Rol et al. assumes that only the collisions of incident beam with atoms near the surface (within the first few monolayers) are important for sputter emission. The ion beam imparts energy to the atoms of the first few atomic layers as it passes through the surface of the solid. The beam then continues into the solid where it is implanted. Although the beam continues to lose energy to the solid as it slows down, it is only the losses to the first few atomic layers that are important for Rol's sputtering model. The energy transferred to the first few atomic layers then institutes collisions among these atoms which cause some to be ejected from the surface. The sputtering

ratio (number of target atoms emitted/incident ion) is found to be proportional to the energy transferred in the first collision and inversely proportional to the mean free path for elastic collisions. The equation obtained by Rol et al. for the sputtering ratio is given by:

$$S = K \frac{1}{\lambda(E) \cos \phi} \frac{M_1 M_2}{(M_1 + M_2)^2} E \quad (1)$$

where M_1 and M_2 are the mass numbers of impinging ion and target atoms, E is energy of impinging particles, K is a constant, ϕ is the angle between the target surface normal and incident beam, and λ is the mean free path for elastic collisions.

Sigmund,³⁰ on the other hand, considers the energy losses of the ion beam throughout its path in the solid. The collisions of incident ions with solid atoms initiate cascades of collisions due to the energetic recoil of the solid atoms. These collision cascades are assumed to be governed by transport theory. When the cascades terminate on a surface atom with enough energy to break the surface bonds, the atom is ejected. Thus,

Sigmund's theory also includes energy transfer of the ion beam within the solid which can cause ejection of surface atoms via energetic recoil atoms and collision cascades.

B. Ion Emission During Ion Bombardment

1. Experimental Data

The sputtering ratios (number of target atoms emitted/incident ion) of pure metals will typically vary less than a factor of 20 at 10 keV incident ion energy.^{1,2} The sputtered ion yields (number of ions emitted from target/total number of target atoms emitted), however, can vary many orders of magnitude.³⁶ This is illustrated in Fig. 1 using an 11 keV $^{16}\text{O}^+$ beam to bombard pure metals.²⁷ The sputtered ion currents noted vary over four orders of magnitude, while the sputtering ratios for these materials typically vary less than a factor of ten. In fact, Au would have a higher sputtering ratio than Al,² yet the sputtered ion intensity is much lower by a factor greater than 10^4 .

The sputtered ion yields are further complicated by the composition of the surface.³⁷ The ion yields of

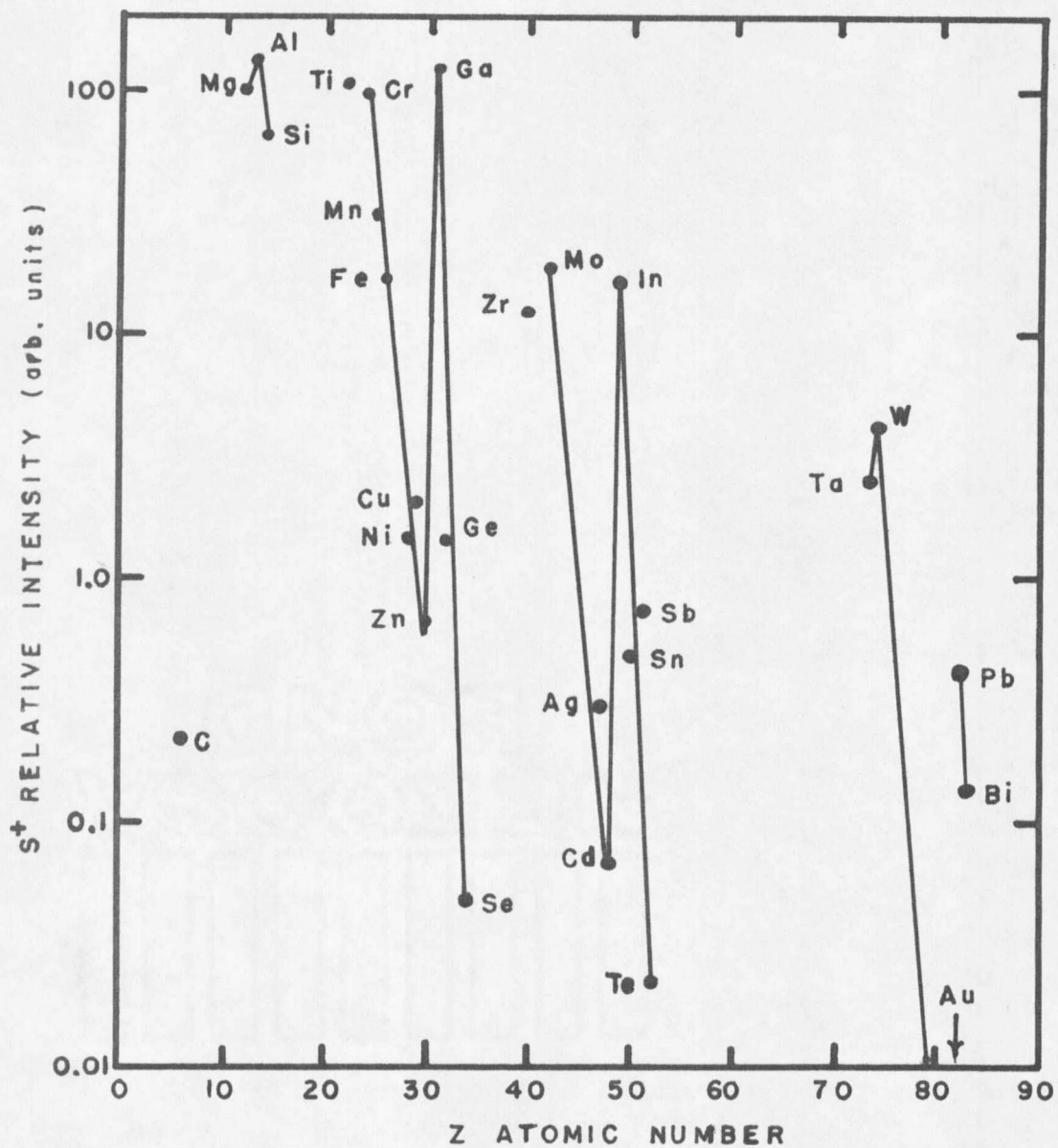


FIG. 1. Illustration of the relative secondary ion currents obtained bombarding pure metals with an 11 keV $^{16}\text{O}^-$ ion beam. (Ref. 27).

elements which have a high affinity for oxygen can be increased by a factor of 10 to 100 by sputtering the oxide of that element instead of the pure element. Likewise, oxide formation can be produced using an oxygen beam to sputter pure elements.³⁷ Thus, when sputter removal reaches the depth of beam implantation,³⁸ the solid surface is then composed of both the original solid elements plus the element of the ion beam. If an oxygen beam is used, the solid's composition will include oxygen.

The energy distribution of the sputtered ions typically has a peak at a few eV but has a high energy tail which can extend to hundreds of eV.³⁹⁻⁴⁴ Recently Ishitani, Tamura and Schinmiyo⁴⁵ have been able to separate the energy distributions of sputtered surface ions from bulk ions. The results indicate that the kinetic energy distribution of sputtered bulk ions can be higher by several tens of an eV than surface ions.

2. Quantum Mechanical Surface Models

One of the first attempts to explain the sputtered ion yields was presented by Van der Weg and Rol.⁴⁶ They used the surface electronic transition models developed

by Hagstrum,⁴⁷ Fig. 2, to explain surface ionization and neutralization of the sputtered species. Resonance transitions can occur via electron tunneling, which can either neutralize a sputtered ion or create a sputtered ion from a neutral sputtered atom. Likewise, the surface Auger transitions allow the possibility of either ion creation or annihilation. The probability that a particle will escape the surface without undergoing a transition is given by:

$$P \sim \exp(-A/av) \quad (2)$$

where v is the velocity component of the particle perpendicular to the surface, A is the transition rate, and a is the characteristic distance from the surface. The transition probability depends greatly on both the particle velocity and the electronic structure of both the solid surface and the sputtered particles. Others who have more recently used these transitions to explain secondary ion emission results include Cini,⁴⁸ MacDonald,⁴⁹ Benninghoven,⁵⁰ and Van der Weg et al.⁵¹

3. Thermodynamic Models

Thermodynamic models have been developed using

